

ARMY RESEARCH LABORATORY



Development and Application of an Evaluation Method for the WRF Mesoscale Model

by Teizi Henmi, Robert Flanigan, and Richard Padilla

ARL-TR-3657

September 2005

NOTICES

Disclaimers

The findings in this report are not to be construed as an official Department of the Army position unless so designated by other authorized documents.

Citation of manufacturer's or trade names does not constitute an official endorsement or approval of the use thereof.

Destroy this report when it is no longer needed. Do not return it to the originator.

Army Research Laboratory

White Sands Missile Range, NM 88002-5501

ARL-TR-3657

September 2005

Development and Application of an Evaluation Method for the WRF Mesoscale Model

Teizi Henmi, Robert Flanigan, and Richard Padilla

Computational & Information Sciences Directorate

Battlefield Environment Division

REPORT DOCUMENTATION PAGEForm Approved
OMB No. 0704-0188

Public reporting burden for this collection of information is estimated to average 1 hour per response, including the time for reviewing instructions, searching existing data sources, gathering and maintaining the data needed, and completing and reviewing the collection information. Send comments regarding this burden estimate or any other aspect of this collection of information, including suggestions for reducing the burden, to Department of Defense, Washington Headquarters Services, Directorate for Information Operations and Reports (0704-0188), 1215 Jefferson Davis Highway, Suite 1204, Arlington, VA 22202-4302. Respondents should be aware that notwithstanding any other provision of law, no person shall be subject to any penalty for failing to comply with a collection of information if it does not display a currently valid OMB control number.

PLEASE DO NOT RETURN YOUR FORM TO THE ABOVE ADDRESS.

1. REPORT DATE (DD-MM-YYYY) September 2005		2. REPORT TYPE Final		3. DATES COVERED (From - To)	
4. TITLE AND SUBTITLE Development and Application of an Evaluation Method for the WRF Mesoscale Model				5a. CONTRACT NUMBER	
				5b. GRANT NUMBER	
				5c. PROGRAM ELEMENT NUMBER	
6. AUTHOR(S) Teizi Henmi, Robert Flanigan, and Richard Padilla				5d. PROJECT NUMBER	
				5e. TASK NUMBER	
				5f. WORK UNIT NUMBER	
7. PERFORMING ORGANIZATION NAME(S) AND ADDRESS(ES) U.S. Army Research Laboratory Computational and Information Sciences Directorate Battlefield Environment Division (ATTN: AMSRD-ARL-CI-EM) White Sands Missile Range, NM 88002-5501				8. PERFORMING ORGANIZATION REPORT NUMBER ARL-TR-3657	
9. SPONSORING/MONITORING AGENCY NAME(S) AND ADDRESS(ES) U.S. Army Research Laboratory 2800 Powder Mill Road Adelphi, MD 20783-1145				10. SPONSOR/MONITOR'S ACRONYM(S)	
				11. SPONSOR/MONITOR'S REPORT NUMBER(S) ARL-TR-3657	
12. DISTRIBUTION/AVAILABILITY STATEMENT Approved for public release; distribution is unlimited.					
13. SUPPLEMENTARY NOTES					
14. ABSTRACT This report establishes automated methods of obtaining and archiving initialization and time-dependent lateral condition data for the Weather Research and Forecast (WRF) mesoscale model. The data includes Eta forecast data, MADIS surface data, and upper-air sounding data. Statistical analysis methods that compare surface and upper-air data between model calculation and observation have also been established and are described in detail. In this study, the WRF was applied to model domains surrounding the National Training Center in southern California. A set of 24-hr forecast data of 2-way, coupled domains (with grid resolutions of 18 and 6 km) were statistically compared with surface and upper-air observation data.					
15. SUBJECT TERMS mesoscale, statistical evaluation, WRF					
16. SECURITY CLASSIFICATION OF:			17. LIMITATION OF ABSTRACT SAR	18. NUMBER OF PAGES 36	19a. NAME OF RESPONSIBLE PERSON Teizi Henmi
a. REPORT U	b. ABSTRACT U	c. THIS PAGE U			19b. TELEPHONE NUMBER (Include area code) 505-678-3519

Standard Form 298 (Rev. 8/98)
Prescribed by ANSI Std. Z39.18

Contents

List of Figures	iv
Summary	1
1. Introduction	3
2. Model Domains and Physics	4
3. Data	5
3.1 Input Data	6
3.2 Data for Comparison	7
3.2.1 Surface Data	7
3.2.2 Upper-Air Sounding Data	7
4. Reading WRF Output File	7
5. Analysis Program	9
5.1 Wind Velocity Components	9
5.2 Height	9
5.3 Temperature	10
5.4 Dew-Point Temperature	10
5.5 Rotating Horizontal Wind Vector Components	11
6. Comparison with Observed Data	12
6.1 Surface Data	12
6.2 Upper-Air Data	13
7. Statistical Comparison Program	16
7.1 Surface Data	16
7.2 Upper-Air Data	17
8. Comparison Results	18
8.1 Surface Data	18

8.2 Upper-Air Data	21
9. Summary and Conclusion	24
References	25
Acronyms	26
Distribution List	27

List of Figures

Figure 1. WRF model domains covering the NTC in southern California.	4
Figure 2. The locations of Eta grid data (*), surface observation data from the Meteorological Assimilation Data Ingest System (MADIS) (S), and upper-air sounding data (U) in the model domains.	6
Figure 3. A script file designed to read a WRF output file in netCDF format and convert it into ASCII format.	8
Figure 4. Horizontal and vertical grids of the WRF.	9
Figure 4. An example of surface data comparison.	13
Figure 5. An example of a vertical profile comparison between observation and model forecast data	14
Figure 6. Vertical profiles of temperature and dew-point temperature for upper-air sounding data and WRF forecast data for station DRA at 1200 UTC, 23 February 2005.	15
Figure 7. Same as figure 6, except for wind speed and wind direction.	15
Figure 8. A time-series of MD, CC, and AD for temperature.	18
Figure 9. Same as figure 8, except for dew-point temperature.	19
Figure 10. Same as figure 8, except for wind speed.	20
Figure 11. A time-series of RMSVE and MWDDF for domains 1 and 2.	21
Figure 12. Vertical profiles of MD for temperature, dew-point temperature, and wind speed for station NKX for a 12-h forecast period.	22
Figure 13. Vertical profiles of AD of temperature, dew-point temperature wind speed, and wind vector components, u and v , for station NKX for a 12-h forecast period. ...	23

Summary

This report establishes automated methods of obtaining and archiving initialization and time-dependent lateral condition data for the Weather Research and Forecast (WRF) mesoscale model. It also establishes statistical analysis methods that compare WRF forecast data with observation data.

The WRF was applied to the model domains surrounding the National Training Center in southern California. A set of 24-h forecast data of 2-way coupled domains (with grid resolutions of 18 and 6 km) were statistically compared with surface and upper-air observation data. For surface temperature, domain 2 (6-km grid resolution) produced better statistical agreements with the observation data than domain 1 (18-km grid resolution).

For dew-point temperature, there were no significant differences between time-series of statistical parameters for domains 1 and 2. For wind speed and vectors, domain 1 produced statistically better agreements between calculation and observation than domain 2.

Vertical profiles of meteorological parameters were also compared between calculation and observation. From that, the following could be inferred:

- The mean absolute difference (AD) of temperature was about 2 °C throughout the model's vertical depth.
- The ADs for dew-point temperature were substantially greater than 2 °C.
- The ADs of wind speed were 5 m/s or greater, but gradually increased with height.

There were no systematic biases in vertical profiles of temperature, dew-point temperature, and wind speed.

INTENTIONALLY LEFT BLANK.

1. Introduction

The Weather Research and Forecast (WRF) model is a weather forecasting system with fully compressible, non-hydrostatic equations. The WRF version 2 has multiple-nesting capability with one-way and two-way coupling. Details of the WRF version 2 have been described by Skamarock et al. (2005).

In a previous study (Henmi, 2004), forecasting skills of surface meteorological parameters of two mesoscale models, the Mesoscale Model Version 5 (MM5) and WRF version 1.3, were statistically evaluated over two different geographical areas: Utah and western Texas. A triple-nested MM5, with grid resolutions of 45, 15, and 5 km, respectively, was used over the Utah area. The WRF version 1.3, which does not have multiple-nesting capability, was used with a 5-km grid resolution. Over the Utah domain, the WRF domain covered an area similar to the MM5 domain 3.

Using the 40-km Eta forecast data freely available from the National Center of Environmental Prediction (NCEP), forecast calculations of both the MM5 and the WRF were carried out and the results were compared with surface observation data.

Both models tended to over-forecast temperature and dew-point temperature, although the correlation coefficients between forecast and observation were fairly high. The statistical parameters for the MM5 were slightly better than those for the WRF. For both the MM5 and the WRF, the statistical parameters for wind vector components were inferior to those of temperature and dew-point temperature, although the WRF values were slightly better than the MM5 values.

For this study, the model domains of the WRF were set over the area surrounding the National Training Center (NTC) located in southern California (figure 1), in order to accomplish the following objectives:

1. To develop the methods for using and statistical evaluating the WRF.
2. To make a statistical comparison between the WRF forecast output of domains 1 and 2 for surface and upper-air meteorological parameters.

2. Model Domains and Physics

WRF double-nested computational domains, depicted in figure 1, were used.

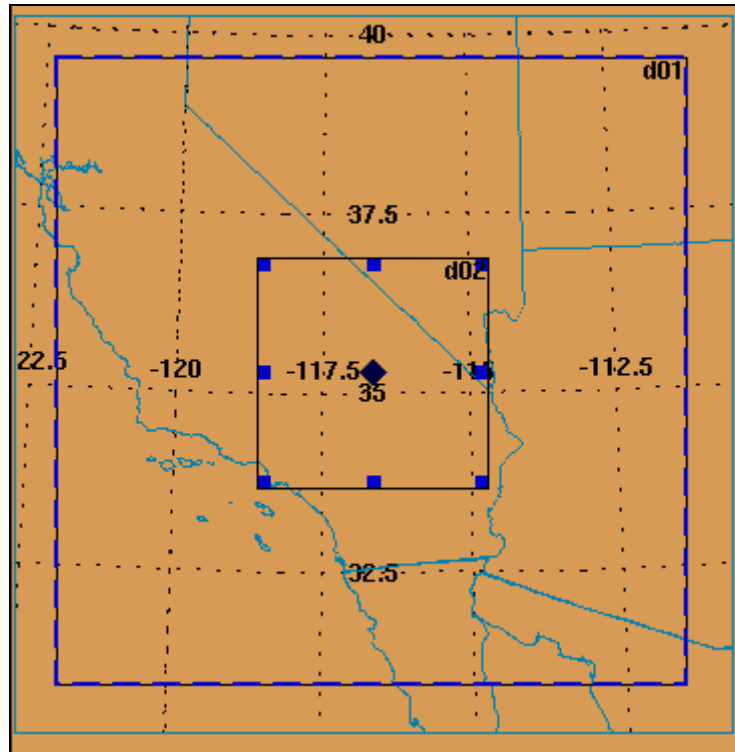


Figure 1. WRF model domains covering the NTC in southern California.

Both domains are centered at 35.30° N. and 116.63° W. Domain 1 has 55-by-55 grid points with an 18-km grid resolution, and domain 2 has 61-by-61 grid points with a 6-km grid resolution. Two-way coupling is used.

The WRF can use a number of different physics options. For this study, the following physics options were used:

- *Planetary boundary layer (PBL)*: A new scheme, known as the Yonsei University PBL, was used. It has an explicit representation of entrainment at the PBL top, which is derived from large eddy simulation modeling. This scheme partially corrects the problem of too much entrainment in the early phase of PBL growth and also adds non-local momentum mixing to provide a realistic wind profile in the PBL (Dudhia, 2004).
- *Precipitation parameterization*: The WRF single-moment three-class was used (Hong et al., 2004). In this scheme, the ice crystal number concentration is dependent on ice mass content rather than temperature, giving realistic ice crystal concentrations and sizes that are compatible with the fall speeds.

- *Cumulus parameterization*: A modified version of the Kain-Fritsch (1990, 1993) was selected. This scheme utilizes a simple cloud model with moist updrafts, including the effects of detrainment, entrainment, and cloud microphysics. A minimum entrainment rate is imposed to suppress widespread convection in marginally unstable, relatively dry environments. Shallow (non-precipitating) convection is allowed for any updraft that does not reach minimum cloud depth for precipitating clouds; this cloud depth varies as a function of cloud-base temperature. In this version, the entrainment is allowed to vary as a function of low-level convergence.
 - *Radiation parameterization*: For long-wave radiation, the rapid radiative transfer model (RRTM) (Mlawer et al., 1997) was used. The RRTM is a spectral-band scheme that uses preset tables to accurately represent long wave processes due to water vapor, ozone, CO₂, and trace gases (if present), as well as accounts for cloud optical depth. For short-wave radiation, a scheme based on Dudhia (1989) was used.
 - *Ground temperature scheme*: The five-layer, soil temperature model used in the MM5 was used for the WRF as well.
-

3. Data

The following datasets are necessary for forecast computation in the WRF and for comparison with the model output. Automated methods to obtain and archive data have been developed.

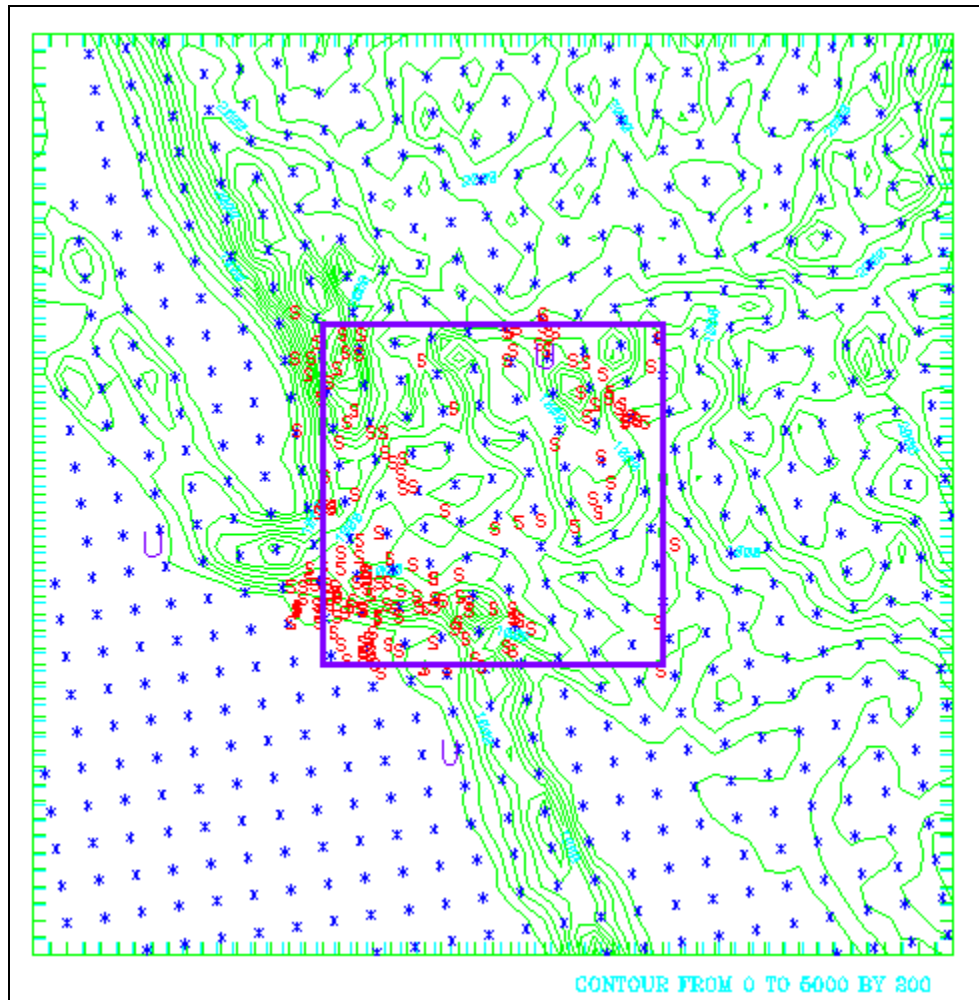


Figure 2. The locations of Eta grid data, surface observation data from the Meteorological Assimilation Data Ingest System (MADIS), and upper-air sounding data in the model domains.

NOTE: * = Eta grid data, S = surface observation data, and U = upper-air sounding data. Terrain contour lines are drawn at every 200 m in height.

3.1 Input Data

Forecast data by a large-scale forecast model are required for initialization and time-dependent lateral condition data to run the WRF.

An automated method to obtain and archive the 40-km Eta (now North American Mesoscale (NAM)) model data in a gridded binary (GRIB) format was developed, and the data was archived for future use. The data are freely available from the NCEP FTP site: <ftp://ftp.ncep.noaa.gov>.

3.2 Data for Comparison

3.2.1 Surface Data

Hourly surface meteorological data are obtained from the Meteorological Assimilation Data Ingest System (MADIS) of the National Oceanic and Atmospheric Administration (NOAA) Forecast System Laboratory (FSL) (<http://www-sdd.fsl.noaa.gov/MADIS>).

Daily data are produced by assembling hourly data for a forecasting period. The data file contains the name of the station, latitude (ϕ_s), longitude (ψ_s), and meteorological parameter value (x_s). Temperature, dew-point temperature, wind speed, and wind direction data are also included in the file.

An automated method to obtain MADIS data has been developed, and daily data consisting of hourly datasets have been archived.

3.2.2 Upper-Air Sounding Data

Upper-air sounding data are obtained from the archive library on the University of Wyoming, Atmospheric Sciences Department's Web site:
<http://weather.uwyo.edu/upperair/sounding.html>.

4. Reading WRF Output File

The WRF produces only one output file in the netCDF format (<http://www.unidata.ucar.edu>) and contains many time-dependent, two-dimensional, and three-dimensional meteorological parameters.

For the current approach, the forecasted parameters necessary for our use were converted from netCDF to ASCII format so that the analysis program could easily read them.

Figure 3 is an example of a script file designed to read a WRF output file in netCDF format and convert it into an ASCII file.

```

# Dumping WRF output data to ascii files for Surface.
# 2-D parameters
# Q2, QV at 2m
ncdump -v Q2 wrfout_d02_2004-10-07_12:00:00>Q2_wrf.file
# T2 Temperature at 2 m
ncdump -v T2 wrfout_d02_2004-10-07_12:00:00>T2_wrf.file
# TH2, Potential temperature at 2 m
ncdump -v TH2 wrfout_d02_2004-10-07_12:00:00>TH2_wrf.file
# U10, U at 10 m
ncdump -v U10 wrfout_d02_2004-10-07_12:00:00>U10_wrf.file
# V10, V at 10 m
ncdump -v V10 wrfout_d02_2004-10-07_12:00:00>V10_wrf.file
# HGT, Terrain height
ncdump -v HGT wrfout_d02_2004-10-07_12:00:00>HGT_wrf.file
# XLAT, Latitude
ncdump -v XLAT wrfout_d02_2004-10-07_12:00:00>XLAT_wrf.file
# XLONG, Longitude
ncdump -v XLONG wrfout_d02_2004-10-07_12:00:00>XLONG_wrf.file
# RAINC, Accumulated total cumulus precipitation (mm)
ncdump -v RAINC wrfout_d02_2004-10-07_12:00:00>RAINC_wrf.file
#
# 3-D parameters
# Pressure
ncdump -v P wrfout_d02_2004-10-07_12:00:00>P_wrf.file
# PB, Base state pressure at half levels
ncdump -v PB wrfout_d02_2004-10-07_12:00:00>PB_wrf.file
# Water Vapor
ncdump -v QVAPOR wrfout_d02_2004-10-07_12:00:00>QVAPOR_wrf.file
# Perturbation geopotential
ncdump -v PH wrfout_d02_2004-10-07_12:00:00>PH_wrf.file
# Base state geopotential
ncdump -v PHB wrfout_d02_2004-10-07_12:00:00>PHB_wrf.file
# U, U wind
ncdump -v U wrfout_d02_2004-10-07_12:00:00>U_wrf.file
# V, V wind
ncdump -v V wrfout_d02_2004-10-07_12:00:00>V_wrf.file
# T, Perturbation potential temp.
ncdump -v T wrfout_d02_2004-10-07_12:00:00>T_wrf.file

```

Figure 3. A script file designed to read a WRF output file in netCDF format and convert it into ASCII format.

In figure 3, “ncdump” is a netCDF program. For instance, “ncdump -v P wrfout-d02-2004-10-07_12:00:00>P_wrf.file” means to read the data of parameter P from the *wrfout-d02-2004-10-07_12:00:00* file and write the data onto the *P_wrf.file* file in ASCII format. Here, the WRF is initialized at 1200 UTC, 07 October 2004 and the data is for the domain 2.

Running this script produces one file for each parameter.

5. Analysis Program

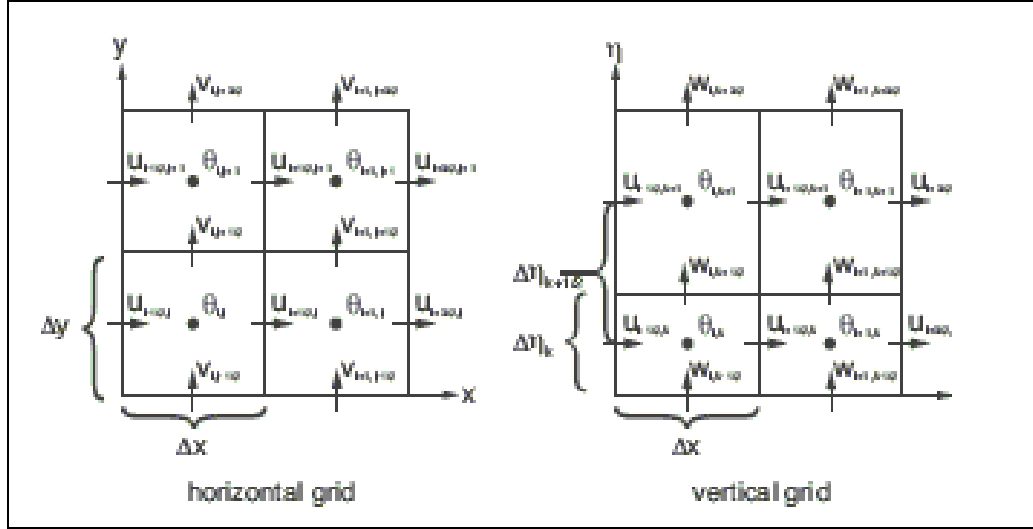


Figure 4. Horizontal and vertical grids of the WRF.

The WRF uses a C grid staggering for variables, as shown in figure 4 (Skamarock, 2005). In the grid, velocity components (u, v, w) are staggered at one-half grid length from the thermodynamic variable θ .

5.1 Wind Velocity Components

Given the grid location of potential temperature θ by (i, j, k, t), wind vector components u, v, and w at (i, j, k) are calculated by

$$u(i, j, k, t) = 0.5(u(i-1/2, j, k, t) + u(i+1/2, j, k, t)) \quad (1)$$

$$v(i, j, k, t) = 0.5(v(i, j-1/2, k, t) + v(i, j+1/2, k, t)) \quad (2)$$

$$w(i, j, k, t) = 0.5(w(i, j, k-1/2, t) + w(i, j, k+1/2, t)) \quad (3)$$

5.2 Height

The WRF output file contains base state and perturbation geopotentials (Φ and Φ'). Vertical height $Z(i, j, k, t)$ is calculated by

$$Z(i, j, k, t) = (\Phi(i, j, k, t) + \Phi'(i, j, k, t)) / g \quad (4)$$

where g is the gravitational acceleration (9.81 m/s^2).

5.3 Temperature

In the model, potential temperature is used as a temperature variable, but for comparison with observed data, it is convenient to use temperature. The WRF output file contains the perturbation potential temperature θ' from 300 °K,

$$\Theta = \theta' + 300.0. \quad (5)$$

Pressure P is the sum of the base state pressure P_B and the perturbation pressure P' :

$$P = P_B + P'. \quad (6)$$

Thus, temperature T is calculated as

$$T = \theta \left(\frac{P}{P_0} \right)^\kappa - 273.16 \quad (7)$$

where P_0 is standard pressure (1,000 mb) and

$$\kappa = \frac{R_d}{C_p} \quad (8)$$

where R_d is the gas constant for dry air and C_p is the specific heat at constant pressure.

5.4 Dew-Point Temperature

The moisture variable in the WRF is expressed by a mixing ratio, but in observational data, the moisture variable is usually given in terms of dew-point temperature

To calculate dew-point temperature from the WRF output mixing ratio, the following steps are taken:

1. Tetan's empirical formula of mixing ratio Q (g/kg) is given as (Yamada and Bunker, 1989)

$$Q = \frac{3.8002}{P} \cdot \exp \left[\frac{T_d - 273.16}{T_d - 35.86} \right] \quad (9)$$

where Q is the mixing ratio (g/kg), P is pressure (mb), and T_d is dew-point temperature (°K).

2. From equation 9, the dew-point temperature is derived as

$$T_d = \frac{35.86xA - 17.27x273.16}{A - 17.27} \quad (10)$$

where A is given by

$$A = \log \left[\frac{PxQ}{3.8002} \right]. \quad (11)$$

5.5 Rotating Horizontal Wind Vector Components

Since the horizontal wind vector components u and v in the WRF output file are along the model coordinate system, they are rotated to the west-to-east and the south-to-north components.

In our applications, the Lambert conformal mapping system was used as a model coordinate system. The following procedures were taken to rotate from (u, v) to (u_t, v_t) . Here (u, v) are the x - and y -components of the horizontal wind vector of the model coordinate, and (u_t, v_t) are the true west-east and south-north components of the horizontal vector.

Let us express the latitude and longitude of grid points by $\phi(i, j)$ and $\psi(i, j)$, and the center latitude and longitude of the model domain by ϕ_c and ψ_c .

A constant for model domain, cone is defined as

$$cone = \sin(|\phi_c|). \quad (12)$$

For each grid point, $\Delta\psi = \psi(i, j) - \psi_c$ is calculated.

For $\Delta\psi > 180.0$,

$$\Delta\psi = \Delta\psi - 360.0. \quad (13)$$

For $\Delta\psi \leq -180.0$,

$$\Delta\psi = \Delta\psi + 360.0. \quad (14)$$

If $\phi(i, j) \leq 0.0$

$$\alpha = -\Delta\psi \cdot cone \quad (15)$$

and for $\phi(i, j) > 0.0$

$$\alpha = \Delta\psi \cdot cone. \quad (16)$$

Horizontal wind vector components (u_t, v_t) are calculated as

$$u_t = v * \sin(\alpha) + u * \cos(\alpha) \quad (17)$$

and

$$v_t = -v * \cos(\alpha) + u * \sin(\alpha). \quad (18)$$

After these calculations, the WRF forecast output data are compared with surface and upper-air observation data for statistical evaluation.

6. Comparison with Observed Data

6.1 Surface Data

The program checks if the latitude and longitude (φ_s and ψ_s) of an observation station is within the model domain and surrounded by four grid points of the model. If surrounded, the model value of an arbitrarily parameter X_m , corresponding to X_s , is computed using the following:

$$X_1 = X(i, j) + \frac{(X(i+1, j) - X(i, j))}{(\psi(i+1, j) - \psi(i, j))} * (\psi_s - \psi(i, j)) \quad (19)$$

$$X_2 = X(i, j+1) + \frac{(X(i+1, j+1) - X(i, j+1))}{(\psi(i+1, j+1) - \psi(i, j))} * (\psi_s - \psi(i, j+1)) \quad (20)$$

$$X_m = X_1 + \frac{(X_2 - X_1)}{(\varphi(i-1, j+1) - \varphi(i, j))} (\varphi_s - \varphi(i, j)) \quad (21)$$

Figure 4 shows an abbreviated table of comparison, showing station names, latitudes, and longitudes, as well as interpolated and observed values for temperature, dew-point temperature, and the horizontal wind components. Values for wind components— u_m and u_s , and v_m and v_s —are recorded in columns 4 through 7.

2 376	Temperature						
AP156		34.86	-118.17	15.6	14.4		
AP263		34.30	-118.51	13.4	14.4		
CEKC1		34.27	-118.15	9.3	8.3		
CNAC1		33.88	-117.55	15.4	15.5		
CTL1		34.32	-117.84	4.5	4.4		
GMT1		34.64	-118.41	11.0	6.1		
CMP12		36.11	-115.15	15.6	15.9		
OWENS		36.80	-118.20	5.0	11.3		
UP013		36.50	-114.76	-999.0	16.6		
UP183		35.66	-115.36	13.1	12.8		
OWENS		36.80	-118.20	5.0	10.5		
2 344	Dew Pt Temp						
AP156		34.86	-118.17	2.1	5.2		
AP263		34.30	-118.51	8.9	9.4		
AP516		36.03	-115.02	4.3	5.5		
AP541		33.87	-117.83	11.3	8.0		
CMP12		36.11	-115.15	4.5	2.3		
OWENS		36.80	-118.20	2.0	0.6		
OWENS		36.80	-118.20	2.0	1.3		
2 356	Wind component						
AP156		34.86	-118.17	2.2	2.5	2.2	2.5
AP263		34.30	-118.51	3.5	2.2	2.9	1.6
AP516		36.03	-115.02	0.2	-0.9	0.2	-2.0
AP541		33.87	-117.83	2.9	0.9	0.5	0.3
ONYC1		35.67	-118.06	2.3	1.4	1.0	1.7
CMP12		36.11	-115.15	0.8	-0.7	0.3	-0.8
OWENS		36.80	-118.20	0.7	-1.2	-0.4	2.4
OWENS		36.80	-118.20	0.7	0.0	-0.4	1.8

Figure 4. An example of surface data comparison.

6.2 Upper-Air Data

In order to make a comparison between vertical profiles of upper-air sounding data and model forecast data, the following procedures are taken:

1. The vertical data of the four grid points surrounding the location of an upper-air sounding station are interpolated to the heights of the sounding data.
2. At each height of sounding data, the bilinear interpolation method described in equations 19 through 21 is used to obtain the vertical profile of the model forecast corresponding to observed upper-air sounding data.

Figure 5 shows a portion of the file containing a vertical profile comparison between observation and model forecast data. The first line shows the latitude and longitude of an upper-air station. The second line shows that there are 52 vertical levels of observation. Column 1 is the height above sea level for the upper-air observation. Columns 2 through 9 are for observation, showing pressure, temperature, dew-point temperature, wind vector the u and v wind components, relative humidity, wind direction, and wind speed. Columns 10 through 14 are for the WRF model forecast, showing pressure, temperature, dew-point temperature, and the u and v wind components.

Figures 6 and 7 show the vertical profiles of upper-air sounding data and interpolation data from model output for station DRA (Mercury, NV) at 1200 UTC, 23 February 2005.

```

36.610006 -116.010002
52
Z      POBS   TOBS   TDOBS  UOBS   VOBS  RHOB   MDOB   MSOBS  PWRF   TWRF   TDWRF  UWRF   VWRF
1009.0  899.0   13.2    1.2   -4.5    2.6  44.0  120.0   5.1 -999.0 -999.0 -999.0 -999.0 -999.0
1149.0  884.0   10.6   -1.4   -3.4    1.2  43.0  110.0   3.6 -999.0 -999.0 -999.0 -999.0 -999.0
1219.0  876.5   10.0   -1.6   -3.0    0.8  44.0  105.0   3.1 -999.0 -999.0 -999.0 -999.0 -999.0
1471.0  850.0    7.8   -2.2   -2.5   -0.7  49.0   75.0   2.6  849.5    8.0   -1.2   -1.8   -1.6
1829.0  813.1    4.5   -3.1   -2.9   -1.1  58.0   70.0   3.1  813.2    4.8   -1.9   -1.8   -1.0
2134.0  783.0    1.6   -3.9   -3.3   -1.5  67.0   65.0   3.6  783.2    1.9   -2.5   -1.6   -0.8
2438.0  754.0   -1.3   -4.7   -4.2   -2.0  78.0   65.0   4.6  754.1   -1.0   -3.4   -1.3   -1.0
2677.0  732.0   -3.5   -5.3   -5.3   -2.0  87.0   69.0   5.7  731.8   -3.2   -5.0   -1.4   -1.5
2743.0  725.9   -3.9   -6.6   -5.3   -1.9  81.0   70.0   5.7  725.7   -3.7   -5.7   -1.5   -1.7
2808.0  720.0   -4.3   -7.9   -5.3   -1.9  76.0   70.0   5.7  719.8   -4.3   -6.3   -1.6   -1.8
3029.0  700.0   -6.3   -8.6   -6.3   -2.3  84.0   70.0   6.7  699.9   -6.0   -8.7   -1.9   -2.2
3048.0  698.3   -6.4   -8.7   -6.8   -2.5  84.0   70.0   7.2  698.2   -6.1   -8.9   -1.9   -2.2
3487.0  660.0   -9.1  -11.0   -6.5   -1.5  86.0   77.0   6.7  659.9   -9.2  -13.2   -2.5   -2.3
3605.0  650.0   -9.7  -14.7   -6.6   -1.3  67.0   79.0   6.7  650.0  -10.0  -14.4   -2.6   -2.2
3658.0  645.6  -10.0  -15.4   -6.6   -1.2  65.0   80.0   6.7  645.5  -10.3  -15.0   -2.6   -2.2
4018.0  616.0  -12.3  -20.3   -7.1   -0.9  51.0   83.0   7.2  616.0  -12.7  -18.7   -1.8   -2.3
4257.0  597.0  -13.1  -18.1   -7.2   -0.6  66.0   85.0   7.2  596.8  -14.3  -21.2   -0.8   -2.6
4267.0  596.2  -13.2  -19.1   -7.2   -0.6  61.0   85.0   7.2  596.0  -14.4  -21.3   -0.8   -2.6
4360.0  589.0  -13.9  -28.9   -7.2   -0.3  27.0   88.0   7.2  588.9  -15.1  -22.3   -0.7   -2.9
4516.0  577.0  -15.3  -28.3   -6.7    0.4  32.0   93.0   6.7  576.8  -16.2  -24.0   -0.5   -3.3
4572.0  572.7  -15.8  -24.6   -6.7    0.6  47.0   95.0   6.7  572.5  -16.6  -24.6   -0.5   -3.4
4621.0  569.0  -16.3  -21.3   -6.7    0.4  65.0   93.0   6.7  568.7  -16.9  -25.1   -0.4   -3.5
4701.0  563.0  -16.7  -31.7   -7.2    0.1  26.0   91.0   7.2  562.7  -17.5  -25.9   -0.5   -3.7
4877.0  549.8  -18.2  -32.1   -7.7   -0.7  28.0   85.0   7.7  549.8  -18.8  -27.7   -0.6   -3.8
5378.0  514.0  -22.3  -33.3   -5.4   -1.8  36.0   71.0   5.7  513.8  -22.7  -32.4   -0.7   -3.8
5522.0  504.0  -23.5  -28.0   -4.7   -2.0  66.0   67.0   5.1  503.8  -23.9  -33.8   -0.8   -3.7
5580.0  500.0  -23.9  -32.9   -4.2   -2.0  43.0   65.0   4.6  499.8  -24.4  -34.3   -0.8   -3.7
5727.0  490.0  -25.1  -39.1   -4.3   -1.7  26.0   68.0   4.6  489.7  -25.5  -35.6   -0.8   -3.6
6096.0  465.0  -28.2  -41.7   -5.0   -1.3  26.0   75.0   5.1  465.5  -28.7  -38.9   -1.1   -3.4
7160.0  400.0  -37.3  -49.3   -5.3   -1.9  28.0   70.0   5.7  400.0  -37.8  -47.6   -2.1   -2.7
7620.0  373.7  -41.5  -52.4   -4.6   -3.2  30.0   55.0   5.7  374.2  -41.9  -50.9   -2.1   -2.1
8439.0  331.0  -48.9  -57.9   -6.0   -1.3  34.0   78.0   6.2  331.2  -48.8  -56.5   -1.2   -0.8
8839.0  311.3  -51.4  -60.4   -6.7    0.0  33.0   90.0   6.7  311.3  -51.8  -59.1   -0.2   -0.2
9080.0  300.0  -52.9  -61.9   -5.6   -0.5  33.0   85.0   5.7  300.4  -52.6  -60.6    1.7   -0.2
9144.0  297.0  -53.2  -62.2   -5.1   -0.9  33.0   80.0   5.1  297.5  -52.9  -61.0    2.2   -0.2
9343.0  288.0  -54.3  -63.3   -4.5   -1.2  32.0   75.0   4.6  288.5  -53.6  -62.2    3.7   -0.3
10250.0 250.0  -54.9  -63.9   -0.6   -0.8  32.0   35.0   1.0  250.8  -53.6  -64.9    9.9   -0.4
10484.0 241.0  -54.7  -64.7    0.4   -2.0  28.0  350.0   2.1  241.8  -52.9  -64.9   11.4   -0.5
10668.0 234.2  -53.5  -63.8    1.8   -1.8  27.0  315.0   2.6  234.7  -52.3  -64.9   12.5   -0.5
10973.0 223.4  -51.4  -62.2    5.3   -1.9  26.0  290.0   5.7  223.6  -51.7  -64.9   13.8   -0.4
11101.0 219.0  -50.5  -61.5    5.3   -2.0  26.0  291.0   5.7  219.5  -51.7  -64.9   13.8   -0.3
11582.0 203.4  -51.8  -62.8    5.6   -2.6  26.0  295.0   6.2  204.1  -51.8  -64.9   13.9    0.3
11690.0 200.0  -52.1  -63.1    5.6   -2.6  25.0  295.0   6.2  200.7  -51.8  -64.9   14.0    0.4
11887.0 194.0  -52.2  -63.4    6.7   -0.6  25.0  275.0   6.7  194.4  -51.9  -64.9   14.0    0.6
12192.0 185.1  -52.3  -63.8    9.2   -0.8  24.0  275.0   9.3  185.3  -52.1  -64.9   14.3    0.5
"upper-air_example" 55L, 5277C

```

Figure 5. An example of a vertical profile comparison between observation and model forecast data

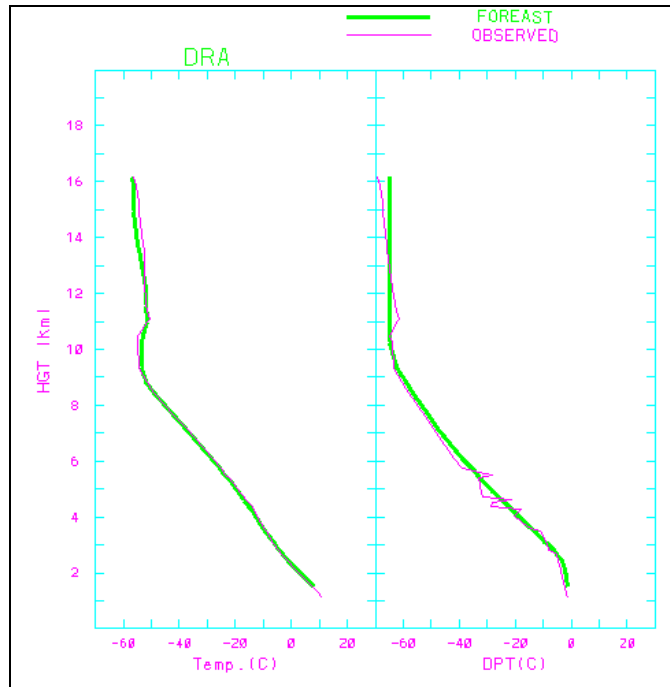


Figure 6. Vertical profiles of temperature and dew-point temperature for upper-air sounding data and WRF forecast data for station DRA at 1200 UTC, 23 February 2005.

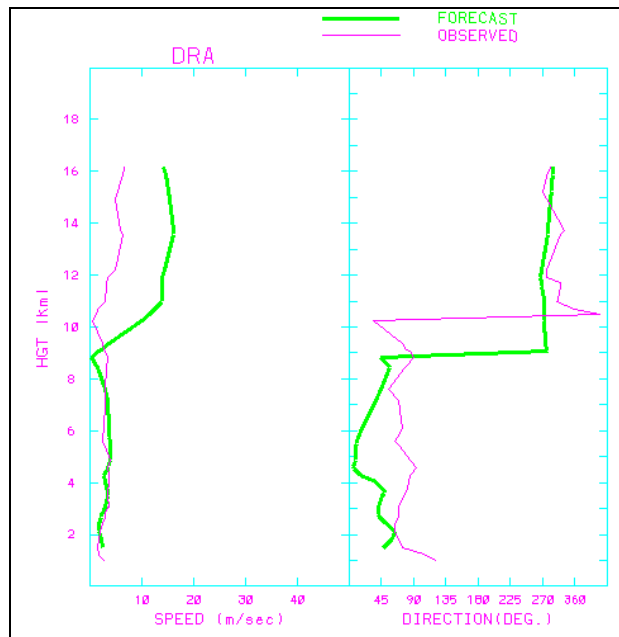


Figure 7. Same as figure 6, except for wind speed and wind direction.

7. Statistical Comparison Program

After files, such as those shown in figures 4 and 5, are produced for numerous different forecast periods, statistical comparison studies can be made between the observation and forecast data.

7.1 Surface Data

In this study, statistical parameters are used to compare observation and model forecast data of temperature and dew-point temperature at the 2-m level, and horizontal wind vector components, u and v , at the 10-m level. Such statistical parameters are calculated hourly.

Mean Difference (MD)

MD is expressed as

$$MD = \frac{\sum_{j=1}^m \sum_{i=1}^n (x_{p,i,j} - x_{o,i,j})}{mn} \quad (22)$$

where the subscripts o and p represent observation and prediction, respectively; the subscript i represents the i^{th} surface station; the subscript j represents the j^{th} forecast day; n is the number of surface stations; and m is the total number of forecast days.

A nonzero MD indicates bias. For instance, if the MD value is positive, it indicates that the model tends to over-forecast.

Mean Absolute Difference (AD)

AD is expressed as

$$AD = \frac{\sum_{j=1}^m \sum_{i=1}^n |x_{p,i,j} - x_{o,i,j}|}{mn} \quad (23)$$

Root Mean Square Error (RMSE)

RMSE is expressed as

$$RMSE = \sqrt{\frac{\sum_{j=1}^m \sum_{i=1}^n (x_{p,i,j} - x_{o,i,j})^2}{mn}} \quad (24)$$

Good agreements between observation and forecast are, in general, related to small values of AD and RMSE.

Root Mean Square Vector Error (RMSVE)

RMSVE is calculated using

$$RMSVE = \sqrt{\frac{\sum_{j=1}^m \sum_{i=1}^n [(u_{p,i,j} - u_{o,i,j})^2 + (v_{p,i,j} - v_{o,i,j})^2]}{mn}}. \quad (25)$$

This parameter measures the differences of both wind speed and wind direction. Good agreements of wind vectors are related to small values of the RMSVE.

Correlation Coefficient (CC)

CC is expressed as

$$CC = \frac{\sum_{j=1}^m \sum_{i=1}^n (y_{p,i,j} * y_{o,i,j})}{\sqrt{\sum_{j=1}^m \sum_{i=1}^n y_{p,i,j}^2 * y_{o,i,j}^2}} \quad (26)$$

where

$$y_{p,i,j} = x_{p,i,j} - \overline{x_p} \quad (27)$$

$$y_{o,i,j} = x_{o,i,j} - \overline{x_o} \quad (28)$$

$$\overline{x_p} = \frac{\sum_{j=1}^m \sum_{i=1}^n x_{p,i,j}}{mn} \quad (29)$$

$$\overline{x_o} = \frac{\sum_{j=1}^m \sum_{i=1}^n x_{o,i,j}}{mn} \quad (30)$$

7.2 Upper-Air Data

Upper-air comparison data, such as shown in figure 6, are calculated at heights specific to each sounding. For statistical evaluation, it is necessary to use data interpolated to pre-defined heights. Using a linear interpolation method, both observed and forecasted data are computed at pre-defined heights.

MD and AD are calculated for each pre-defined height for upper-air sounding stations located within the model domain.

8. Comparison Results

WRF forecast calculations were intermittently carried out during a period from December 10, 2004 to February 28, 2005. Thirty-three 24-h forecast calculations were made during that time.

8.1 Surface Data

The forecast data from domains 1 and 2 were compared with the MADIS surface observation data. A comparison was made each hour during a 24-h forecast period. Figure 8 shows a time-series of MD, CC, and AD for temperature during a 24-h period.

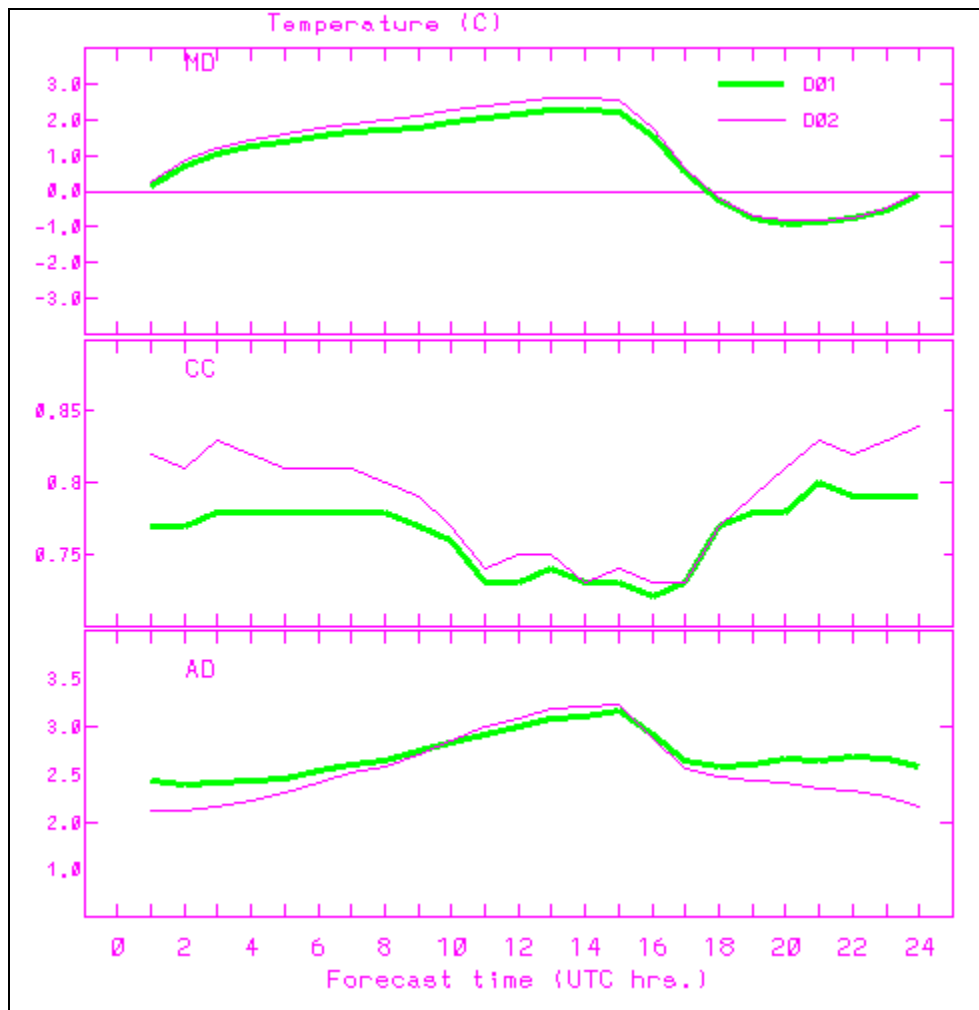


Figure 8. A time-series of MD, CC, and AD for temperature.

NOTE: The thick lines are for domain 1 and the thin lines are for domain 2.

Although the time-series of MD of temperature for domain 2 is slightly greater than that for domain 1, the time-series of CC and AD show that the forecast output of domain 2 produced better agreements with the observation data than those of domain 1.

A time-series of the statistical parameters for dew-point temperature are shown in figure 9. Contrary to the temperature statistics, the statistics for dew-point temperature show little difference between domains 1 and 2, although there was a slight improvement of AD for domain 2 over domain 1.

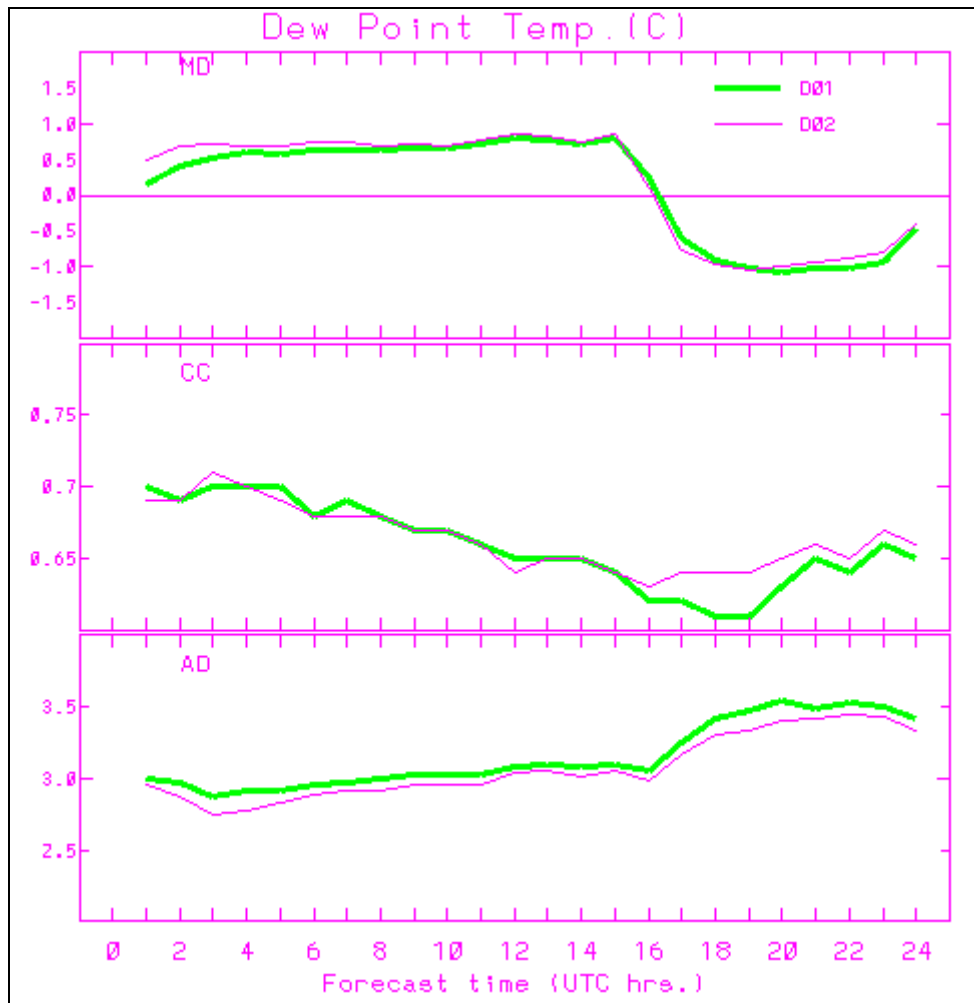


Figure 9. Same as figure 8, except for dew-point temperature.

Figure 10 shows a time-series of MD, CC, and AD for wind speed. MD for domain 1 is smaller than that for domain 2, CC for domain 1 is greater than that for domain 2, and AD for domain 1 is smaller than that for domain 2.

A time-series of RMSVE and MWDDF are shown in figure 11. The values for both RMSVE and MWDDF for domain 1 are smaller than those for domain 2.

Therefore, from figures 10 and 11, it can be inferred that the wind fields of domain 1 are statistically better than those of domain 2.

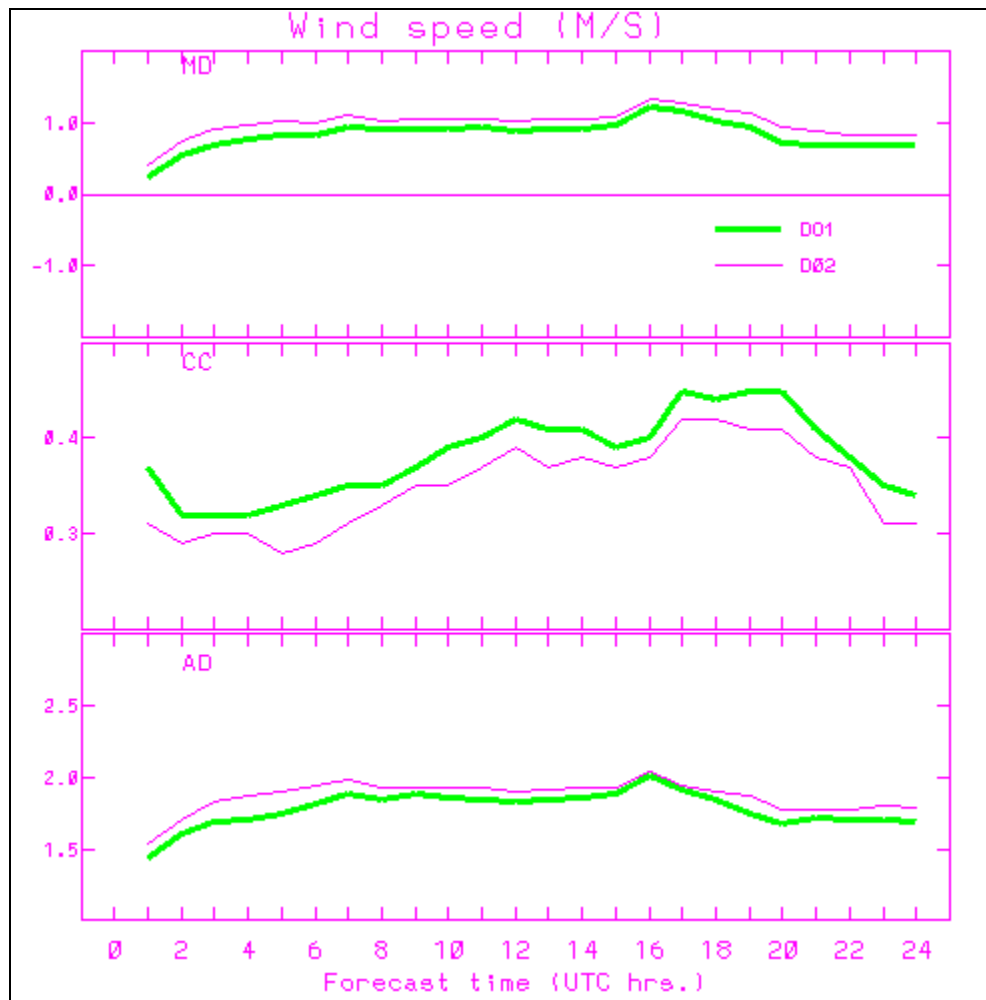


Figure 10. Same as figure 8, except for wind speed.

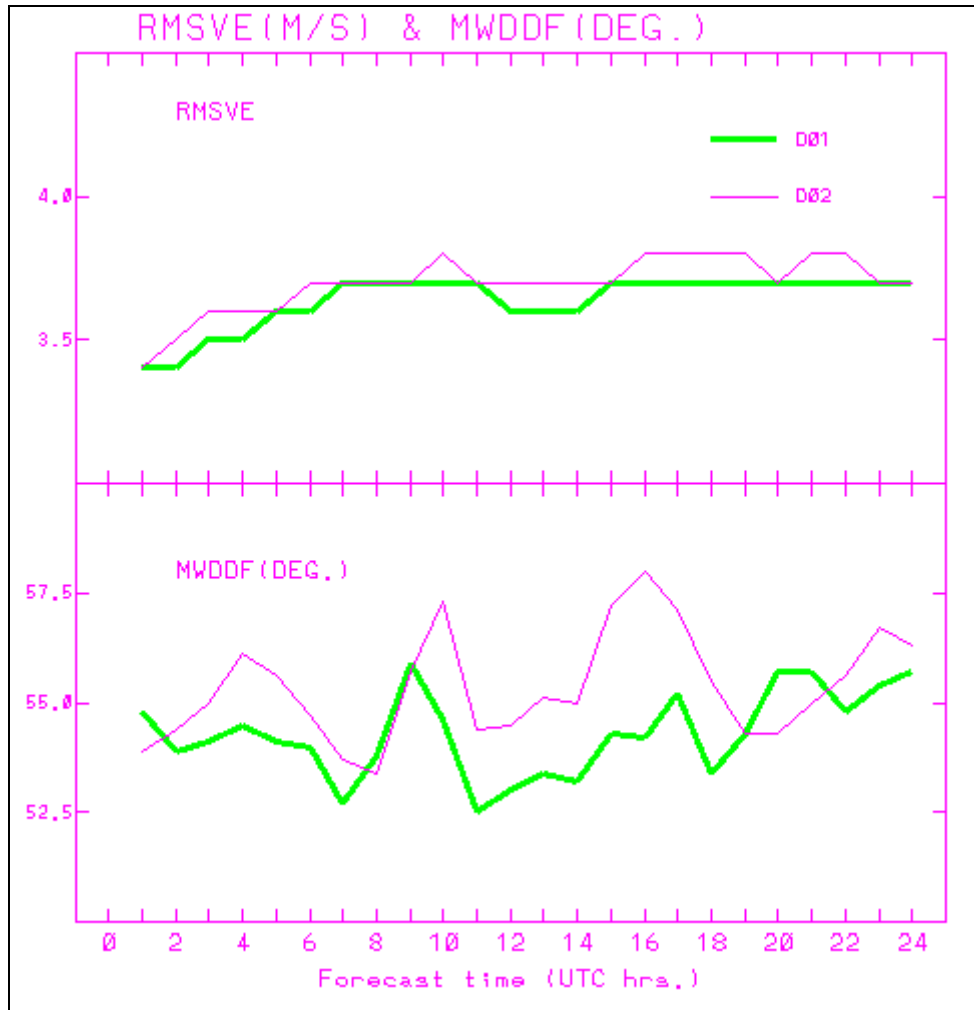


Figure 11. A time-series of RMSVE and MWDDF for domains 1 and 2.

8.2 Upper-Air Data

Vertical profiles of MD and AD are obtained for three upper-air stations—DRA (Mercury, NV), NKX (San Diego, CA), and VBG (Vandenberg Air Force Base, CA)—located within domain 1 (see figure 2). Figure 12 is the vertical profiles of MD for temperature, dew-point temperature, and wind speed for a forecast period of 12-h for NKX. Vertical profiles of AD are also shown in figure 13 for the same time period and station. These are the mean values obtained from 33 different cases.

Similar figures are obtained for the other stations and for different time periods, but are not shown in this report.

Figure 12 shows that the WRF did not significantly over- or under-predict the three variables throughout the vertical layers of the atmosphere for station NKX.

From figure 13, the following can be inferred: the ADs of temperature throughout the vertical layers were 1 to 2 °C, but for dew-point temperature, the ADs were significantly

larger. For wind speed and the wind vector components u and v , the ADs stayed around 5 m/s, but showed a gradual increase with height.

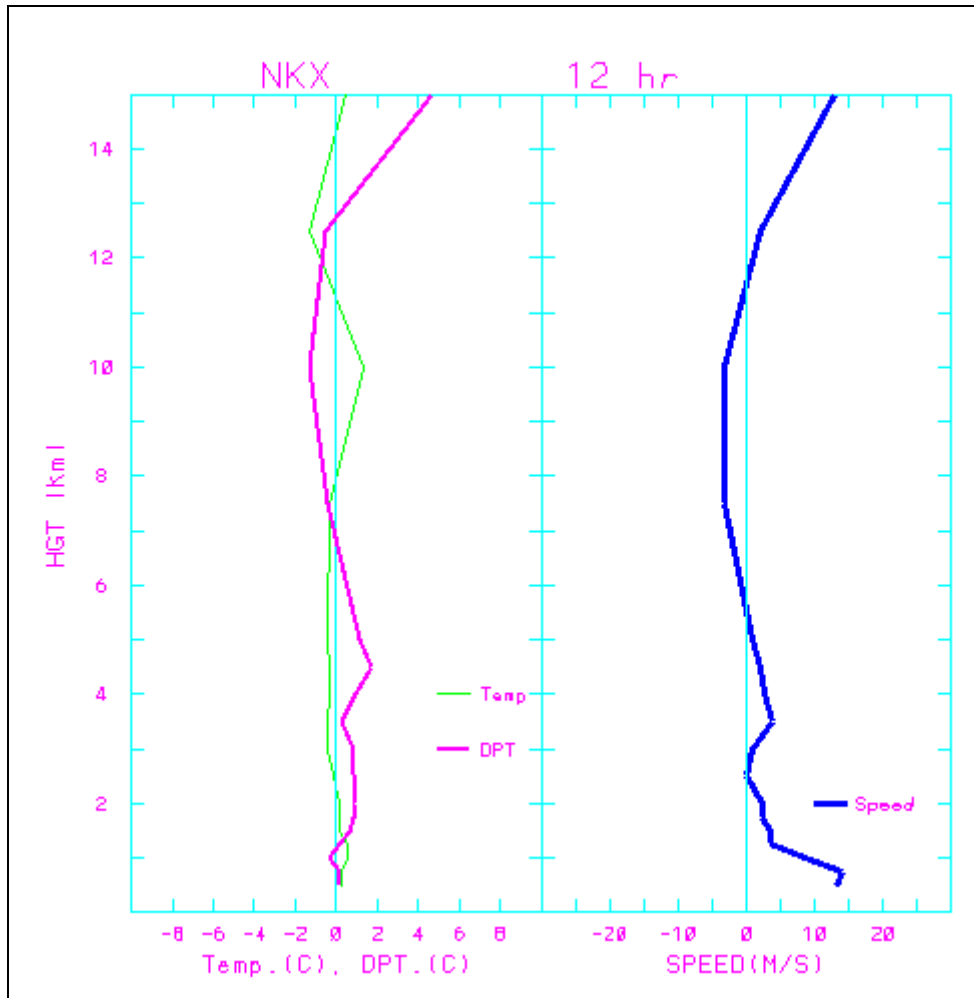


Figure 12. Vertical profiles of MD for temperature, dew-point temperature, and wind speed for station NKX for a 12-h forecast period.

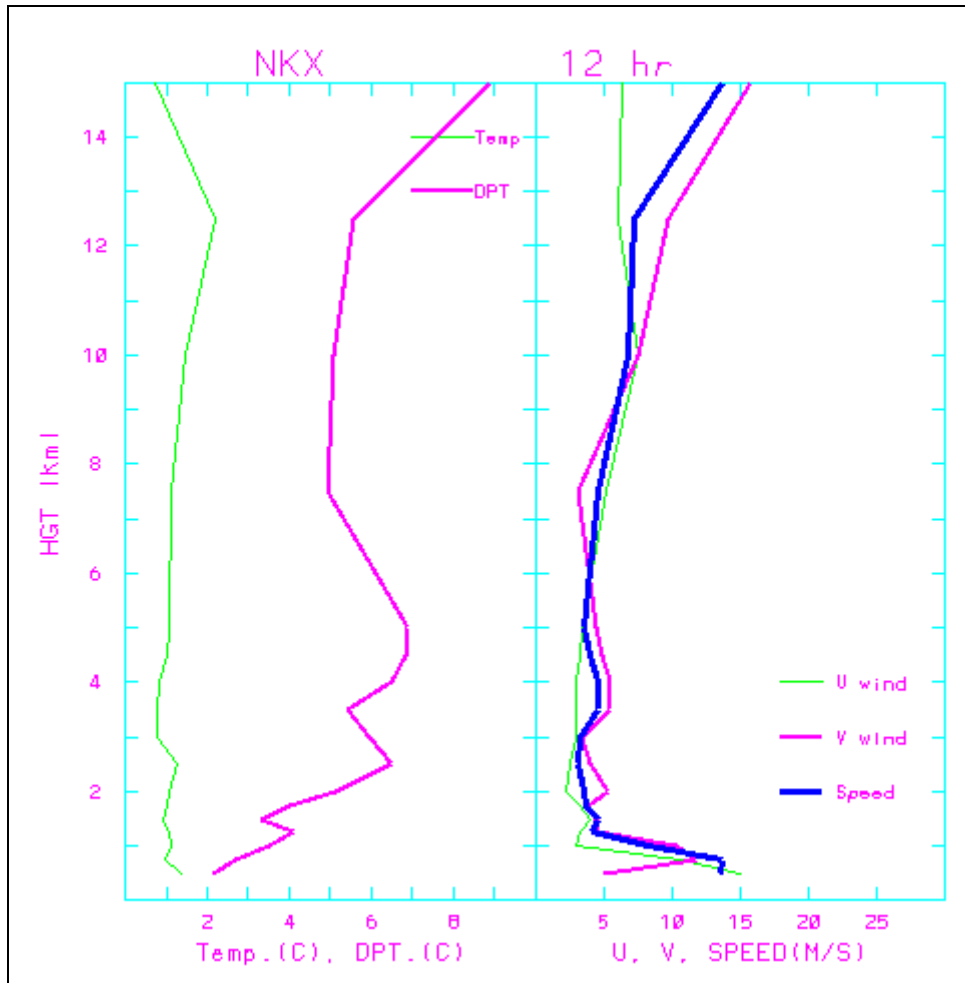


Figure 13. Vertical profiles of AD of temperature, dew-point temperature wind speed, and wind vector components, u and v , for station NKX for a 12-h forecast period.

9. Summary and Conclusion

We have established automated methods of obtaining and archiving initialization and time-dependent lateral condition data for the WRF. These data include Eta (NAM) forecast data, MADIS surface data, and upper-air sounding data.

We also established statistical analysis methods that compare WRF forecast data with observation data. This report described methods of comparing surface as well as upper-air data between model calculation and observation.

The WRF was applied to model domains surrounding the NTC in southern California. In this study, a set of 24-h forecast data of 2-way coupled domains, with the grid resolutions of 18 and 6 km, were statistically compared with surface and upper-air observation data.

For surface temperature, domain 2 (a 6-km grid resolution) produced better statistical agreements with observations than domain 1 (an 18-km grid resolution).

There were no significant differences between time-series of statistical parameters for domains 1 and 2. However, for wind speed and vectors, domain 1 produced statistically better agreements between calculation and observation than domain 2.

Vertical profiles of temperature, dew-point temperature, and wind speed and vector components were compared between calculation and observation. From that the following could be inferred:

- The ADs for temperature were about 2 °C throughout the model's vertical depth.
- The ADs for dew-point temperature were substantially greater than 2 °C.
- The ADs for wind speed were 5 m/s or greater, but gradually increased with height.

There were no systematic biases in vertical profiles of temperature, dew-point temperature, and wind speed.

References

- Dudhia, J. A Numerical Study of Convection Observed During the Winter Monsoon Experiment Using a Mesoscale Two-Dimensional Model. *J. of Atmos. Sci.*, **1989**, *46*, 3077–3107.
- Dudhia, J. *The Weather Research and Forecast Model Version 2.0: Physics Update*, WRF/MM5 Summer Workshop, Extended Abstract, National Center for Atmospheric Research, 2004.
- Henmi, T. Statistical Studies of Mesoscale Forecast Models MM5 and WRF; ARL-TR-3329; U.S. Army Research Laboratory: White Sands Missile Range, NM, 2004.
- Hong, S.Y.; Dudhia, J.; Chen, S.H. A Revised Approach to Ice Microphysical processes for the Bulk Parameterization of Cloud and Precipitation. *Monthly Weather Rev.*, **2004**, *132*, 103.
- Kain, J.S.; Fritsch, J.M. A One-Dimensional Entraining/Detraining Plume Model and its Application in Convective Parameterization. *J. of Atmos. Sci.*, **1999**, *47*, 2784–2802.
- Kain, J.S.; Fritsch, J.M. *Convective Parameterization for Mesoscale Models: The Kain-Fritsch Scheme*. *The Representation of Cumulus Convection in Numerical Models*, K. A. Emanuel and D. J. Raymond, eds.; American Meteorological Society, 1993, p 246.
- Mlawer, E.J.; Taubman, S.J.; Brown, P.D.; Iacono, M.J.; Clough, S.A. Radiative Transfer for Inhomogeneous Atmosphere: RRTM, A Validated Correlated-k Model for the Long-Wave. *J. of Geophysical Res.*, **1997**, *102* (D14) 11163–11182.
- Skamarock, W.C.; Klemp, J.B.; Dudhia, J.; Gill, D.M.; Barker, D.M.; Wang, W.; Powers, J.G. *A Description of the Advanced Research WRF Version 2*; NCAR/TN-468+STR; Mesoscale and Microscale Meteorology Division, National Center for Atmospheric Research: Boulder, CO, 2005.
- Yamada, T.; Bunker, S. A Numerical Model Study of Nocturnal Drainage Flows with Strong Wind and Temperature Gradients. *J. of Applied Meteorology*, **1989**, *82*, 407–430.

Acronyms

AD	absolute difference
CC	correlation coefficient
DRA	Mercury, NV, station
FSL	Forecast System Laboratory
GRIB	Gridded Binary
MADIS	Meteorological Assimilation Data Ingest System
MD	mean difference
MM5	Mesoscale Model Version 5
MWDDF	mean wind direction difference
NAM	North American Mesoscale model
NCEP	National Center of Environmental Prediction
NKX	San Diego, CA, station
NOAA	National Oceanic and Atmospheric Administration
NTC	National Training Center
PBL	planetary boundary layer
RMSVE	root mean square vector error
RRTM	Rapid Radiative Transfer Model
VBG	Vandenberg Air Force Base, CA, station
WRF	Weather Research and Forecast model

Distribution List

	Copies
US ARMY RESEARCH LAB AMSRD ARL CI BE ATTN T HENMI R FLANIGAN R PADILLA WSMR NM 88002-5501	3
US ARMY RESEARCH LAB ATTN IMNE ALC IMS MAIL & RECORDS MGMT ADELPHI MD 20783-1197	1
ADMNSTR DEFNS TECHL INFO CTR ATTN DTIC OCP ELECT CPY V MADDOX 8725 JOHN J KINGMAN RD STE 0944 FT BELVOIR VA 22060-6218	1
US ARMY RESEARCH LAB AMSRD ARL CI OK TL TECHL LIB 2800 POWDER MILL ROAD ADELPHI MD 20783-1197	2
US ARMY RESEARCH LAB AMSRD CI OK TP TECHL LIB APG MD 21005	1
TOTAL	8

INTENTIONALLY LEFT BLANK.

